



# A New Method of Target Detection Based on Autonomous Radar and Camera Data Fusion

2017-01-1977

Published 09/23/2017

**Xin Bi, Bin Tan, and Zhijun Xu**

Tongji Univ.

**Libo Huang**

Automotive Sensors Group

**CITATION:** Bi, X., Tan, B., Xu, Z., and Huang, L., "A New Method of Target Detection Based on Autonomous Radar and Camera Data Fusion," SAE Technical Paper 2017-01-1977, 2017, doi:10.4271/2017-01-1977.

Copyright © 2017 SAE International

## Abstract

Vehicle and pedestrian detection technology is the most important part of advanced driving assistance system (ADAS) and automatic driving. The fusion of millimeter wave radar and camera is an important trend to enhance the environmental perception performance. In this paper, we propose a method of vehicle and pedestrian detection based on millimeter wave radar and camera. Moreover, the proposed method complete the detection of vehicle and pedestrian based on dynamic region generated by the radar data and sliding window. First, the radar target information is mapped to the image by means of coordinate transformation. Then by analyzing the scene, we obtain the sliding windows. Next, the sliding windows are detected by HOG features and SVM classifier in a rough detect. Then using the match function to confirm the target. Finally detecting the windows in a precision detection and merging the detecting windows. The target detection process is carried out in the following three steps. The first step is to read the radar signal and capture the camera data at the same time. The second step is to frame and fuse the data. The third step is to detect the target and display the result. Through experiments, it is proved that the fusion algorithm we proposed can detect vehicle and pedestrian better, and provide the basis for the following target tracking research.

## Introduction

In traffic accidents, there is a large proportion of accidents caused by rear end collision, of which 91% of rear end accidents are caused by distraction of drivers. So vehicle and pedestrian detection technology has become an important part of advanced driver assistance systems (ADAS). It is used to accurately identify vehicles and pedestrians ahead, timely remind the driver before the risk of collision, and prevent the happening of the accident.

In vehicle and pedestrian detection, using a single sensor is often faced with the problem of the high rate of false detection and missed detection. However, the speed and accuracy of vehicle and pedestrian detection can be improved by fusing information of radar and camera.

In the fusion of vehicle detection based on millimeter wave radar and camera, Shigeki Sugimoto et al [1] has completed the transformation from radar to the camera coordinate and annotated information on the image, but no further work was done. Giancarlo Alessandretti et al [2], Trung - Dung Vu et al [3] and li-sheng jin et al [4], JIN Lisheng [5] have completed fusion algorithm and test the vehicle, but no further research has been done on the region generated by radar. In the pedestrian detection based on fusion of millimeter wave radar and camera, because of the limited ability of early millimeter wave radar to detect pedestrians, little research has been done. At present, millimeter wave radar can meet the requirements of pedestrian detection, and can be integrated with the camera for pedestrian detection.

Aiming to make up for the shortage of the single sensor detection, and study radar and camera fusion detection in detail, this paper proposes a new method of radar and camera fusion. This algorithm uses the radar target information to determine dynamic region generated by the radar data in image. Then by analyzing the scene to get dynamic sliding windows. Next, the sliding windows can be test through the HOG features and SVM classifier in a rough detect. Then using the match function to confirm the target. Finally detecting the windows in a precision detection and merging the detecting windows.

## Coordinate Fusion

### Conversion of Coordinates

Radar and camera are sensors in different coordinate systems. Therefore, to realize the spatial fusion of sensors, the coordinates of the two sensors need to be unified. Therefore, it is necessary to build a transition relation between radar coordinate system and image pixel coordinate system.

Figure 1 shows the relative position of the millimeter-wave radar coordinate system  $O_r R_r \theta_r$ , camera coordinate system  $O_c - X_c Y_c Z_c$  and 3D world coordinate system  $O_w - X_w Y_w Z_w$ . In this paper, we set that the world coordinate system coincides with camera coordinate system.

As shown, the installation position of millimeter wave radar and camera is fixed. Therefore, plane  $O_r R_r \theta_r$  is perpendicular to the plane  $X_c O_c Z_c$ . So the camera coordinate system  $P(X_c, Y_c, Z_c)$  and radar system  $P(R_r, \theta_r)$  transformational relation is shown below:

$$\begin{bmatrix} X_c \\ Y_c \\ Z_c \\ 1 \end{bmatrix} = \begin{bmatrix} 0 & -1 & 0 & L_x \\ 0 & 0 & 0 & L_y \\ 1 & 0 & 0 & L_z \\ 0 & 0 & 0 & 0 \end{bmatrix} \begin{bmatrix} R_r \cos \theta_r \\ R_r \sin \theta_r \\ 0 \\ 1 \end{bmatrix} \quad (1)$$

Where  $L_x, L_y, L_z$  are the distances between the camera coordinate system and the radar coordinate system in three directions.

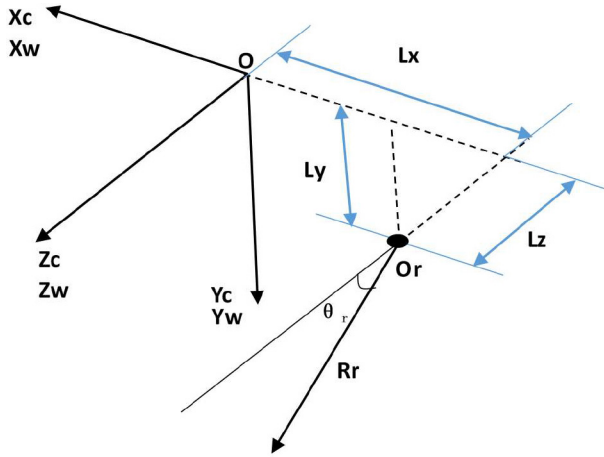


Figure 1. The relative position of three coordinate systems.

And the transformation formula from the camera coordinate system  $P(X_c, Y_c, Z_c)$  to the image pixel coordinate system  $(u, v)$  is:

$$Z_c \begin{bmatrix} u \\ v \\ 1 \end{bmatrix} = \begin{bmatrix} \frac{1}{d_x} & 0 & u_0 \\ 0 & \frac{1}{d_y} & v_0 \\ 0 & 0 & 1 \end{bmatrix} \begin{bmatrix} f & 0 & 0 & 0 \\ 0 & f & 0 & 0 \\ 0 & 0 & 1 & 0 \end{bmatrix} \begin{bmatrix} X_c \\ Y_c \\ Z_c \\ 1 \end{bmatrix} \quad (2)$$

In the above equation, the  $d_x$  and  $d_y$  represent the physical length of each pixel in the X axis and the Y axis in the image pixel coordinate system, the pixel coordinates  $(u_0, v_0)$  is the intersection point of the optical axis  $Z_c$  and the image plane,  $f$  is the focal length of camera.

The transformation relation between radar coordinate system and image pixel coordinate system can be obtained by the formula (1) and the formula (2):

$$Z_c \begin{bmatrix} u \\ v \\ 1 \end{bmatrix} = M_1 M_2 M_3 \begin{bmatrix} R_r \cos \theta_r \\ R_r \sin \theta_r \\ 0 \\ 1 \end{bmatrix} \quad (3)$$

In above:

$$M_1 = \begin{bmatrix} \frac{1}{d_x} & 0 & u_0 \\ 0 & \frac{1}{d_y} & v_0 \\ 0 & 0 & 1 \end{bmatrix} \begin{bmatrix} f & 0 & 0 & 0 \\ 0 & f & 0 & 0 \\ 0 & 0 & 1 & 0 \end{bmatrix}$$

$$M_2 = \begin{bmatrix} 1 & 0 & 0 & 0 \\ 0 & 1 & 0 & 0 \\ 0 & 0 & 1 & 0 \\ 0 & 0 & 0 & 1 \end{bmatrix}$$

$$M_3 = \begin{bmatrix} 0 & -1 & 0 & L_x \\ 0 & 0 & 0 & L_y \\ 1 & 0 & 0 & L_z \\ 0 & 0 & 0 & 0 \end{bmatrix}$$

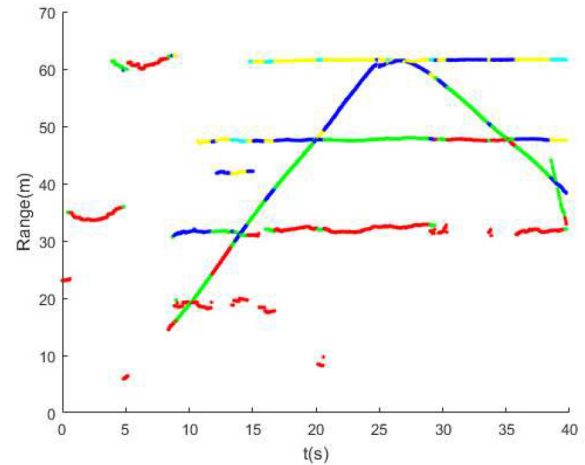
Among them,  $M_1$  is the internal parameter matrix of the camera,  $M_2$  is the transformation matrix from the world coordinate system to the camera coordinate system,  $M_3$  is the transformation matrix from the radar coordinate system to the world coordinate system.

## The Region Generated by Radar Data

The region generated by radar is used for matching the target generated by camera. Since in radar targets the miss rate is much less than the false positives rate and the camera detection has a better accuracy in detecting the target, the camera target in the region generated by radar have a better credibility in fusion.

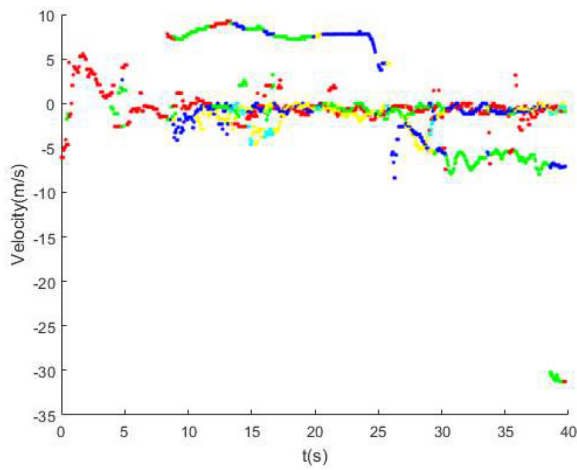
## Radar Signal Preprocessing

As shown in Figure 2, the graph of the original range, velocity and angle can be got by drawing raw data of the target distance of radar output over time. Meanwhile, the radar target signal can be converted to the image and get the converted raw data diagram. The radar target information can continuously output the trajectory of the target. At the same time, all obstacles will be exported, including the roadside guardrail, telephone poles, trees, etc. In addition, some false targets will be exported.

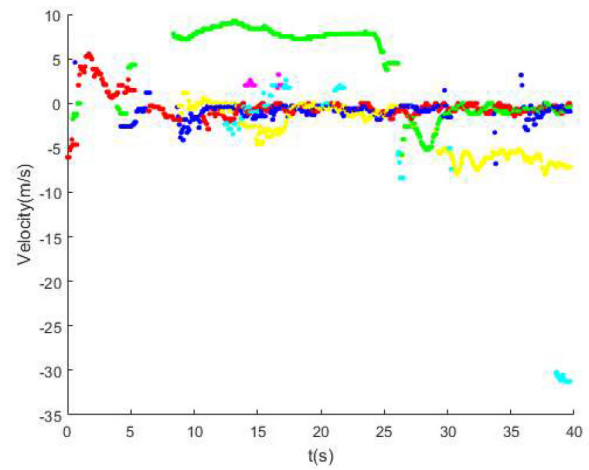


a. Original range data for radar output.

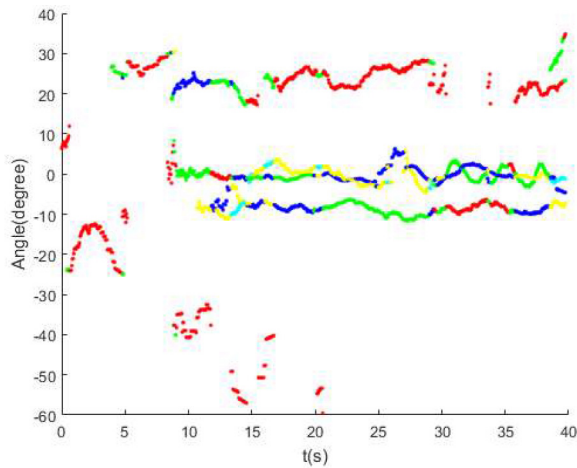
Figure 2. Original data for radar output.



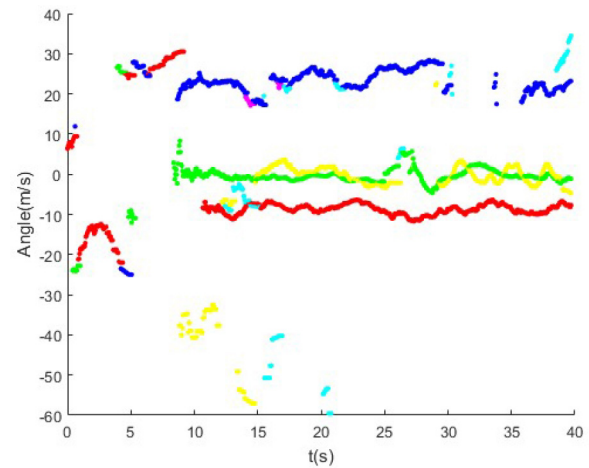
b. Original velocity data for radar output.



b. Velocity data for radar output after filtering.



c. Original angle data for radar output.



c. Angle data for radar output after filtering.

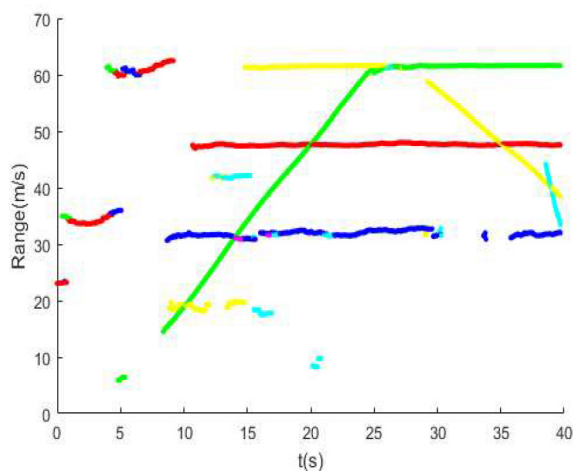
Figure 2 (cont). Original data for radar output.

Figure 3. Data for radar output after filtering.

The false target can be filtered by filtering and tracking radar data. For other obstacles, we can use the method of image detection to judge. After tracking filtering of radar data, the figure of target information can be obtained. Figure 3 shows the output data (including range, velocity, and angle) of radar after filtering. Then we can convert the radar signal of one radar cycle to the image and get the fusion figure in Figure 4. And the white area in the figure is the transformed area.



Figure 4. The fusion figure of radar and camera.



a. Range data for radar output after filtering.

### Calculate the Region Generated by Radar Data

The calculation of the region generated by Radar includes the position and area size. This paper gives a new method for determination of the region by certification and considering multiple factors.

Firstly, the pretreatment radar target ( $R_r, \theta_r$ ) is mapped to the image by coordinate transformation in the previous section. Then the corresponding points  $O_1$  can be got in the image. Theoretically, that

point is located at the center of the target contour in the image so that this point is used as the center of the region generated by radar in vehicle detection.

Considering the actual installation, the horizontal angle of the camera is consistent with the roll angle of the vehicle. The region generated by radar in the world coordinate system can be determined as the rectangular region which center is the radar target, and the rectangular region is perpendicular to the vertical axis.

According to GB 159-2016, the limit of the outline of the vehicle in wide  $W_m$  is 2.55 m, and in height  $H_m$  is 4 m. This size can meet the detection requirements for most cars, trucks or other vehicles.

So select the test area should consider the angular resolution of the radar  $\alpha$ , radar range resolution  $L$ , the distance between radar and the world coordinate system and angle measurement error.

The test area selected is following:

$$\begin{bmatrix} X_l \\ X_l \\ Z_l \\ 1 \end{bmatrix} = M_4 M_5 \begin{bmatrix} (R_r - L) \cos(\theta_r + \alpha) \\ (R_r - L) \sin(\theta_r + \alpha) \\ 1 \\ 1 \end{bmatrix} + \begin{bmatrix} \frac{W_m}{2} \\ \frac{H_m}{2} \\ -L \\ 0 \end{bmatrix} \quad (4)$$

$$\begin{bmatrix} X_r \\ Y_r \\ Z_r \\ 1 \end{bmatrix} = M_6 M_7 \begin{bmatrix} (R_r - L) \cos(\theta_r - \alpha) \\ (R_r - L) \sin(\theta_r - \alpha) \\ 1 \\ 1 \end{bmatrix} + \begin{bmatrix} \frac{W_m}{2} \\ \frac{H_m}{2} \\ -L \\ 0 \end{bmatrix} \quad (5)$$

$$M_4 = \begin{bmatrix} 1 & 0 & 0 & 0 \\ 0 & \cos \beta_x & -\sin \beta_x & 0 \\ 0 & \sin \beta_x & \cos \beta_x & 0 \\ 0 & 0 & 0 & 0 \end{bmatrix} \begin{bmatrix} \cos \beta_y & 0 & -\sin \beta_y & 0 \\ 0 & 1 & 0 & 0 \\ \sin \beta_y & 0 & \cos \beta_y & 0 \\ 0 & 0 & 0 & 0 \end{bmatrix} \begin{bmatrix} 0 & -1 & 0 & L_x - P_x \\ 0 & 0 & 0 & L_y - P_y \\ 1 & 0 & 0 & L_z - P_z \\ 0 & 0 & 0 & 0 \end{bmatrix} \quad (6)$$

$$M_5 = \begin{bmatrix} 1 & 0 & 0 & 0 \\ 0 & \cos \beta_x & \sin \beta_x & 0 \\ 0 & -\sin \beta_x & \cos \beta_x & 0 \\ 0 & 0 & 0 & 0 \end{bmatrix} \begin{bmatrix} \cos \beta_y & 0 & \sin \beta_y & 0 \\ 0 & 1 & 0 & 0 \\ -\sin \beta_y & 0 & \cos \beta_y & 0 \\ 0 & 0 & 0 & 0 \end{bmatrix} \begin{bmatrix} 0 & -1 & 0 & L_x + P_x \\ 0 & 0 & 0 & L_y + P_y \\ 1 & 0 & 0 & L_x + P_x \\ 0 & 0 & 0 & 0 \end{bmatrix} \quad (7)$$

Where  $\beta_x, \beta_y$  represent measurement error in the clockwise rotation angle in the  $Y_c Z_c$  and  $Z_c X_c$  plane between camera coordinate system and radar system.  $P_x, P_y, P_z$  are measurement error in 3 directions.  $[X_l$

$Y_l Z_l], [X_r Y_r Z_r]$  are respectively the lower left and right corner coordinates of the interested area in camera coordinate system.  $M_4$  is the matrix when the measurement error is considered that caused to the most distant way between the upper left corner and center in the area generated by radar.  $M_5$  is the matrix when the measurement error is considered that caused to the most distant way between the upper right corner and center in the area generated by radar.

From formula (2), the transformation relationship between radar coordinate system and image pixel coordinate system is:

$$Z_{cl} \begin{bmatrix} u_l \\ v_l \\ 1 \end{bmatrix} = M_1 \begin{bmatrix} X_l \\ X_l \\ Z_l \\ 1 \end{bmatrix} \quad (8)$$

$$Z_{cr} \begin{bmatrix} u_r \\ v_r \\ 1 \end{bmatrix} = M_1 \begin{bmatrix} X_r \\ Y_r \\ Z_r \\ 1 \end{bmatrix} \quad (9)$$

Where  $[u_l v_l], [u_r v_r]$  are the coordinate of upper left corner and lower right corner in area generated by radar in the image pixel coordinate system.

The method to get the dynamic region generated by radar data for pedestrian detection is as same as the method of determining region generated by radar for the vehicle detection. The top limit size of pedestrians profile in wide  $W_p$  is 0.5 m, height  $H_p$  is 2 m. In the same way, through coordinate transformation, the region generated by radar of pedestrian detection can be got in image pixel coordinate system.

## Vision-Based Vehicle and Pedestrian Detection

On the vehicle and pedestrian detection, the algorithm based on machine learning is the more commonly used methods [6]. The kernel technologies of vehicle and pedestrian detection algorithm based on machine learning are feature extraction and classification. Feature extraction methods include Haar-like features, LBP features, edgelet features, SIFT features, HOG features, etc. Classification algorithms include decision tree, neural network, Bayesian classification, support vector machine (SVM), k-nearest neighbor classification algorithm and so on. In the selection of the detection algorithm, the gradient directional histogram (HOG) features can well express the edge of the image, meeting the requirement of pedestrian and vehicle detection [7]. At the same time, support vector machines (SVM) algorithm is a very good classification algorithm, which can classify data by training hyperplane. So we adopt the vehicles and pedestrian detection algorithm based on the HOG characteristics and the SVM classifier. In terms of vehicles and pedestrian detection, this paper focuses on how to use the region generated by radar to detect the vehicle and pedestrian after obtaining the region generated by radar of vehicles and pedestrians.



## Feature Extraction

The gradient directional histogram (HOG) features [8] represent the edge features of the object by computing the gradient information of the local region of the image. It has good invariance in the change of local geometry and optical. And the information of vehicle and pedestrian is mainly the gradient information of the edge part, so it has been widely used in pedestrian and vehicle detection.

For the extraction of HOG features, this paper use the method proposed by Dali et al.

1. Convert the image to grayscale, as shown in [Figure 5](#) & [Figure 6](#).
2. Standardize color space of the input image by using Gamma correction method, adjust image contrast, reduce local shadow and illumination change influence.

Gamma compression formula:

$$I(x, y) = I(x, y)^{\text{gamma}} \quad (10)$$

Advisable gamma=0.5.

3. Calculate gradient and orientation of each pixel, get the image contour information.

The gradient of the pixels (x, y) in the image is:

$$G_x(x, y) = H(x + 1, y) - H(x - 1, y) \quad (11)$$

$$G_y(x, y) = H(x, y + 1) - H(x, y - 1) \quad (12)$$

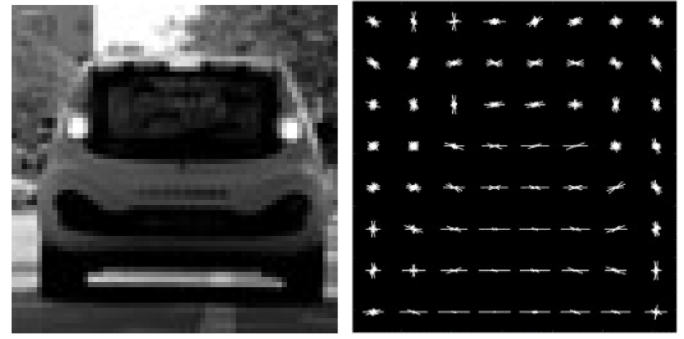
In the formula,  $G_x(x, y)$ ,  $G_y(x, y)$ ,  $H(x, y)$  represent respectively horizontal gradients, vertical gradients, and pixel values of the pixels (x, y) in the input image. The gradient amplitude and gradient directions of pixels (x, y) are:

$$G(x, y) = \sqrt{G_x(x, y)^2 + G_y(x, y)^2} \quad (13)$$

$$\alpha(x, y) = \tan^{-1}\left(\frac{G_y(x, y)}{G_x(x, y)}\right) \quad (14)$$

4. Divide the image into small pieces, called cell.
5. Get each cell histogram statistics, form descriptor of each cell.
6. Each block consists of several cell, including all the cell feature descriptor.
7. All HOG features descriptor of images constitute the feature vector of the image.

In term of vehicle detection, sliding window is scaled to 64 x 64 pixels, each small piece including 8 x 8 pixels. In the direction of gradient, it is divided into nine blocks, a block containing 2 x 2 adjacent cell. The adjacent blocks are overlapping, and the step size is as big as the size of small pieces. At last, the HOG character after transformation is described as the vector of a length of 1764. The vehicle grayscale and its HOG feature maps is shown below:

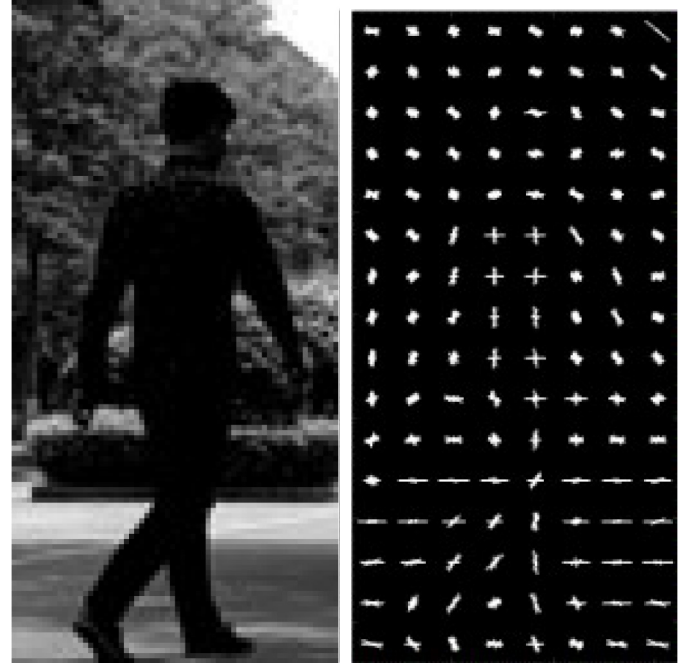


a. Grayscale

b. HOG feature map

Figure 5. Vehicle grayscale and its HOG feature map.

In term of pedestrian detection, sliding window is scaled to 128 x 64 pixels. Other settings are similar to vehicle settings. Finally, the HOG character is described as the vector of a length of 3780. The Pedestrians' grayscale and its HOG feature maps is shown below:



a. Grayscale

b. HOG feature maps

Figure 6. Pedestrians' grayscale and its HOG feature map.

## Training a Support Vector Machine

In the training of support vector machine (SVM), the selection of samples has a great influence on the training results. The larger the number of valid samples, the closer results to reality. Vehicle detection samples are from KITTI [9] and GTI Vehicle Image Database [10] as well as the samples made by ourselves. Positive samples include vehicles on the back and side in road collecting by the car camera. Negative samples include road, lane lines, guardrails, etc.

Pedestrian detection samples are from CVC pedestrian database [11] and some samples made by ourselves. The sample library is used for pedestrian detection in advanced driving assistance system research.

Positive samples include pedestrians in all directions in road area. And negative samples include road area of non- pedestrian area. It accords with the requirements of road pedestrian detection.

The HOG feature vectors of the image are used as the input data of SVM to train the classifier. At the same time, vehicle and pedestrian detection need to strike a balance between high accuracy and speed using linear SVM classification method. So samples are divided into test set by the method of cross validation, and the vehicle and pedestrian detection classifier are trained, respectively.

Finally, the linear SVM discriminant function after training is:

$$f = \text{sgn}(\sum \alpha_i^* y_i^* < x_i^*, x > + b^*) \quad (15)$$

$x^*$  is the support vector,  $\alpha^*$  is the support coefficient,  $b^*$  is the offset.

### Sliding window detection

Sliding -window detection represents a group of windows generated from a single input image source. And the windows have different size for detecting the target in different distances. The windows should cover the maximum range of target size. The detecting windows is shown below, and windows in different colors use detecting target in different distances.

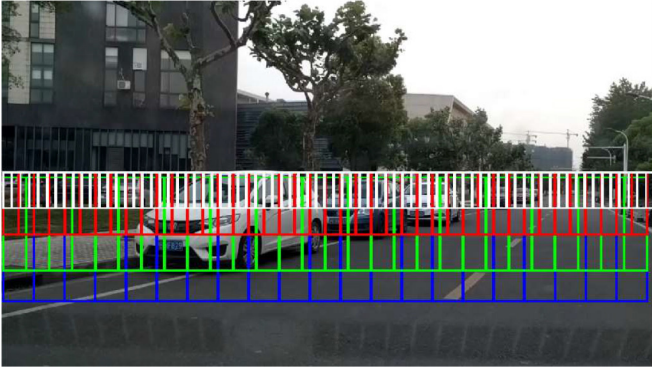


Figure 7. The detecting windows

### Target Fusion

Radar has a high precision in velocity and distance measurement and a limited ability to detect static targets because of the environmental background noise. However, a camera can detect a static or dynamic pedestrian or vehicle in a particular scene. Thus, the target fusion algorithm need take advantage of both.

Figure 8 shows the fusion algorithm chart. The data from radar and camera are fused at a high level. The vision process, detecting vehicle and pedestrian in the sliding windows. Then match the target based in the region generated by the radar. Finally, the fusion system output the results.

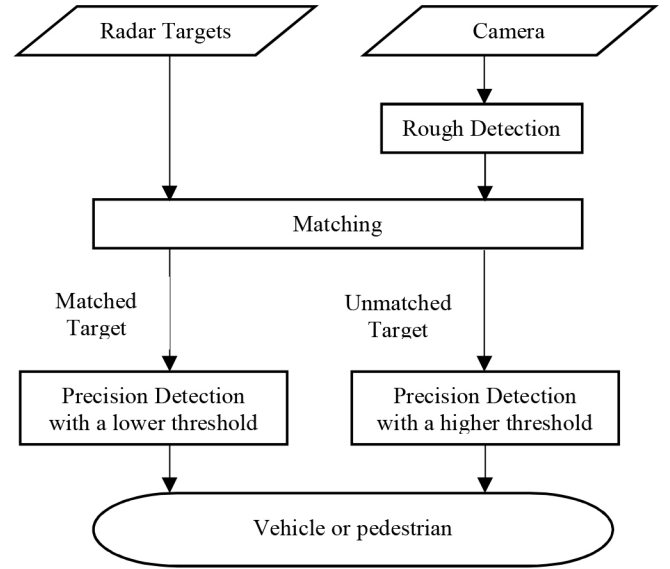


Figure 8. Fusion algorithm flow chart

### Matching

The coordinate of upper left corner and lower right corner of the region generated by radar in the image pixel coordinate system are  $[u_l, v_l]$   $[u_r, v_r]$ . The coordinate of upper left corner and lower right corner of the sliding windows are  $[u_{sl}, v_{sl}]$ ,  $[u_{sr}, v_{sr}]$ .

In fact, the region generated by radar data is not equal to the sliding with the target due to vehicle pitch and non-flat road, while  $[u_l, v_l]$   $[u_r, v_r]$  is not equal to  $[u_{sl}, v_{sl}]$ ,  $[u_{sr}, v_{sr}]$  due to large lateral errors in radar data.

The target in different distance could have different size of the region generated by radar data. Then select the most appropriate box by the matching function.

A simple matching function consider the closeness and the area is defined as:

$$F = C_1 |u_r - u_l - u_{sr} + u_{sl}| + C_2 |v_r - v_l - v_{sr} + v_{sl}| + C_3 \left| \left( \frac{(u_{sr} - u_{sl})(v_{sr} - v_{sl})}{(u_r - u_l)(v_r - v_l)} - 1 \right) \right| \quad (16)$$

Where  $C_1$  and  $C_2, C_3$  are adjustable weight values. In the vision process, all the matching measurements between radar and vision targets after the rough detection are computed and are sorted. Then sort these results and find whether it is greater than the threshold.

### Detection

Two classifications of different scales are trained for rough detection and precision detection. A rough detection classification is able to quickly filter out unreasonable targets, and a precision detection classification can detect vehicles and pedestrians correctly. The difference of the rough detection and the precision detection are the scale of the training and detecting picture. In addition, the matched target will be detected using a precision detection classification with a

lower threshold and the unmatched target will be detected using a precision detection classification with a higher threshold. Finally, by merging and extracting sliding windows the target can be detected.

## Result

Vehicle and pedestrian detection figures can be obtained, as shown in Figure 8 & Figure 9. In addition, the distance and the velocity of the matched target can be get from radar's data.



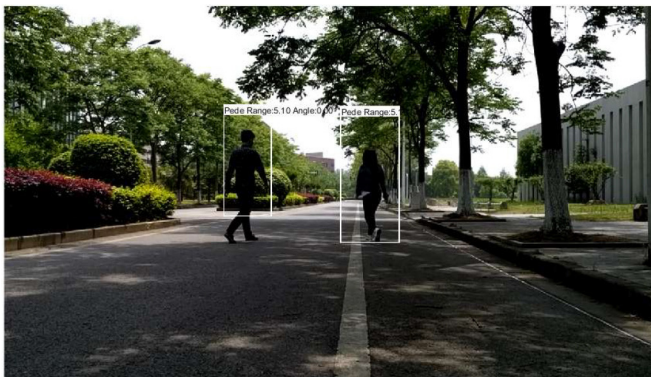
a. Vehicle detection figure.

b. Pedestrian detection figure.

Figure 9. Vehicle and pedestrian detection figures.



a. Detection result of vehicle in experiment.



b. Detection result of pedestrian in experiment.

Figure 10. Detection result in experiment

## Summary

In this paper, we put forward a method of vehicle and pedestrian detection based on radar and camera fusion, and completed the identification of vehicles and pedestrians based on dynamic region and a target fusion algorithm. The test shows that the proposed algorithm can detect the vehicles and pedestrians accurately. Vehicle and pedestrian detection is one of the most important part of the advanced driver-assistance systems. This paper just fuses the data of radar and cameras and detect only vehicles and pedestrians. Therefore, the following work are the research of visual inspection and tracking study based on the fusion algorithm.

## References

1. Sugimoto S, Tateda H, Takahashi H, et al. "Obstacle detection using millimeter-wave radar and its visualization on image sequence." Pattern Recognition, 2004. ICPR 2004. Proceedings of the 17th International Conference on. IEEE, 2004, 3: 342-345.
2. Alessandretti G, Broggi A, Cerri P. "Vehicle and guard rail detection using radar and vision data fusion." IEEE Transactions on Intelligent Transportation Systems, 2007, 8(1): 95-105.
3. Vu T D, Aycard O, Tango F. "Object perception for intelligent vehicle applications: A multi-sensor fusion approach." Intelligent Vehicles Symposium Proceedings, 2014 IEEE. IEEE, 2014: 774-780.
4. Lisheng JIN, Lei CHENG, Bo CHENG. "Leading vehicle detection at night based on millimeter-wave radar and machine vision." Journal of Automobile Safety and Energy Conservation, 2016, 7(02): 167-174.
5. Liu, Xin, Sun Zhenping, and He Hangen. "On-road vehicle detection fusing radar and vision." Vehicular Electronics and Safety (ICVES), 2011 IEEE International Conference on. IEEE, 2011.
6. Kejia ZHOU. "Research on pedestrian detection and tracking based on HOG and template matching." Jilin University, 2014.
7. Pei Ma. "Research on detection technology of HOG feature based vehicle." MS thesis. of South China University of Technology, 2015.
8. Dalal, Navneet, and Triggs Bill. "Histograms of oriented gradients for human detection." Computer Vision and Pattern Recognition, 2005. CVPR 2005. IEEE Computer Society Conference on. Vol. 1. IEEE, 2005.
9. Geiger A, Lenz P, Urtasun R. "Are we ready for autonomous driving? the kitti vision benchmark suite." Computer Vision and Pattern Recognition (CVPR), 2012 IEEE Conference on. IEEE, 2012: 3354-3361.
10. Arróspide J., Salgado L., Nieto M.. "Video analysis based vehicle detection and tracking using an MCMC sampling framework." EURASIP Journal on Advances in Signal Processing, vol. 2012, Article ID 2012:2, Jan. 2012 (doi: 10.1186/1687-6180-2012-2)
11. Gonzalez A., Fang Z., Socarras Y., Serrat J., Vazquez D., Xu J. & Lopez A.. "Pedestrian Detection at Day/Night Time with Visible and FIR Cameras: A Comparison." In Sensors Journal (Sensors), In Press. 2016

## Contact Information

Bin Tan  
Tongji University No.4800 Cao'An Road, Jiading District, Shanghai,  
Republic of China  
[tanbin@tongji.edu.cn](mailto:tanbin@tongji.edu.cn)

## Acknowledgments

National Key R&D Program of China 2016YFB0101101

## Abbreviations

**HOG** - The feature is constructed by calculating histograms of gradient directions of local regions of the image

**SVM** - SVM is based on limited sample information to find the best compromise between model complexity and learning ability in order to achieve the best promotion capability

**ROI** - region of interest

**Haar-like** - The Haar eigenvalue reflects the gray change of the image

**LBP** - LBP is an operator used to describe local texture features of an image

**SIFT** - SIFT is a local feature detection algorithm, the algorithm using the feature points for a picture and the scale and orientation descriptors feature and image feature point matching, and achieved favorable effect,

---

The Engineering Meetings Board has approved this paper for publication. It has successfully completed SAE's peer review process under the supervision of the session organizer. The process requires a minimum of three (3) reviews by industry experts.

All rights reserved. No part of this publication may be reproduced, stored in a retrieval system, or transmitted, in any form or by any means, electronic, mechanical, photocopying, recording, or otherwise, without the prior written permission of SAE International.

Positions and opinions advanced in this paper are those of the author(s) and not necessarily those of SAE International. The author is solely responsible for the content of the paper.

ISSN 0148-7191

<http://papers.sae.org/2017-01-1977>